

PAPER

Moderate pressure plasma source of nonthermal electrons

To cite this article: S Gershman and Y Raitses 2018 *J. Phys. D: Appl. Phys.* **51** 235202

View the [article online](#) for updates and enhancements.

Related content

- [Foundations of DC plasma sources](#)
Jon Tomas Gudmundsson and Ante Hecimovic
- [Atmospheric pressure dc glow discharge](#)
David Staack, Bakhtier Farouk, Alexander Gutsol et al.
- [Foundations of atmospheric pressure non-equilibrium plasmas](#)
Peter J Bruggeman, Felipe Iza and Ronny Brandenburg

Moderate pressure plasma source of nonthermal electrons

S Gershman¹  and Y Raitsev 

Princeton Plasma Physics Laboratory, Princeton, NJ 08540, United States of America

E-mail: sgershma@pppl.gov

Received 15 October 2017, revised 28 March 2018

Accepted for publication 20 April 2018

Published 15 May 2018



Abstract

Plasma sources of electrons offer control of gas and surface chemistry without the need for complex vacuum systems. The plasma electron source presented here is based on a cold cathode glow discharge (GD) operating in a dc steady state mode in a moderate pressure range of 2–10 torr. Ion-induced secondary electron emission is the source of electrons accelerated to high energies in the cathode sheath potential. The source geometry is a key to the availability and the extraction of the nonthermal portion of the electron population. The source consists of a flat and a cylindrical electrode, 1 mm apart. Our estimates show that the length of the cathode sheath in the plasma source is commensurate (~0.5–1 mm) with the inter-electrode distance so the GD operates in an obstructed regime without a positive column. Estimations of the electron energy relaxation confirm the non-local nature of this GD, hence the nonthermal portion of the electron population is available for extraction outside of the source. The use of a cylindrical anode presents a simple and promising method of extracting the high energy portion of the electron population. Langmuir probe measurements and optical emission spectroscopy confirm the presence of electrons with energies ~15 eV outside of the source. These electrons become available for surface modification and radical production outside of the source. The extraction of the electrons of specific energies by varying the anode geometry opens exciting opportunities for future exploration.

Keywords: glow discharge, electron source, non-equilibrium plasma, non-local plasma, nonthermal electrons

(Some figures may appear in colour only in the online journal)

1. Introduction

Glow discharges (GDs) have been investigated and used for over a hundred years, but continue to be subject to investigations due to the continued development of new applications, due to persistent puzzles associated with the detailed structure and behavior, and as a low cost physical model particularly for the study of nonthermal and non-local plasma processes [1–7]. The nonthermal distributions of ions and electrons affect the volume and surface chemistry. However, plasma sources of broad energy spectrum result in activation of competing processes and hence in poor selectivity of the resulting chemical processes. Therefore, the success of chemical applications depends on the precision targeting of specific

molecular transitions for the activation of certain reaction channels or breaking of the specific bonds in the decomposition processes.

In low pressure surface modification, plasmas with prescribed chemical composition can be produced by the use of electron beams [8]. These electron beam sources operate in high or ultra-high vacuum. Recently, these sources have been coupled to fore-vacuum pump pressure chambers for plasma generation or chemical processing by using differential pumping techniques and special membranes between chambers that allow high energy electron beams to pass [8–10]. These are technically complex and costly systems. The production of high energy electrons at higher pressures leads to the formation of plasma between the accelerating electrodes. The space charge then leads to shielding and reduction in the electron energy. Several approaches have been proposed that

¹ Author to whom any correspondence should be addressed.

either attempt to prevent the discharge formation or extract higher energy electrons from the discharge region. The former can possibly produce higher energy electrons ($>100\text{eV}$) while the latter promise higher degree of control over the electron energy distribution function (EEDF) [11, 12].

The non-equilibrium nature of the GD has been long accepted, and the existence of the high energy component of the electron population and depending on the applied voltage, beam electrons, was proposed by Langmuir. The studies of the structure of the GD and the EEDF are still ongoing [1–6, 13–15]. The discharge structure, the spatial distribution of the electric field and the charge density as well as the electron energy distributions have been investigated [13] for GD with $pL \sim 3\text{--}8\text{ torr}\cdot\text{cm}$, where p is the pressure and L is a characteristic size of the discharge. In addition to confirming the non-locality of the GD, the studies developed detailed changes in the charge density and electric field along the axial dimension showing that the sign of the anode sheath is dependent on the density driven reversals of the electric field. The studies in [15] showed that 1D models are insufficient and 2D particle balance is needed for understanding of the GD.

In this work, we investigate a simple dc GD geometry for use as a controllable source of nonthermal electrons with energies $>10\text{eV}$. The geometry of the GD presented here is similar to the plane-to-cylinder geometry of a Grimm-type discharge used historically for the spectroscopic investigations of the cathode material and other analytical applications [16–18]. However, the usual parameters of Grimm-type sources are about an order of magnitude larger in size and have two orders of magnitude higher currents than the source used in this study, hence we expect considerable differences in the characteristics and possible applications of our plasma source. Grimm discharges operated in similar ranges of pressure and applied voltage, have been shown to have plasma density in the $10^{10}\text{--}10^{11}\text{ cm}^{-3}$ range and electron temperature of 1eV or lower. The currents in those discharges are at least an order of magnitude higher than in our arrangements mostly due to the significantly larger sizes and higher applied voltage. As a result, the Grimm discharges are characterized by cathode and gas heating. With gas heating up to $\sim 1000\text{K}$, Grimm discharges are closer to local thermal equilibrium (LTE) [16–18].

Electron beam generation in nanosecond pulsed GD such as an open discharge in He and other noble gases has been used for pumping lasers, in light sources, and other applications that require high intensity electron beams in gas environments. These discharges are generated between a cold cathode and a single-hole or multi-hole mesh anode with an interelectrode distance of about 1mm and $pL < 5\text{ torr}\cdot\text{cm}$. Extensive studies attribute the electron generation to the photoemission from the cathode in the pulsed regime with an added contribution of secondary emission due to the bombardment of the cathode by gas atoms and ions in a continuous or quasi-continuous regimes [19–22]. Many investigations focused on optimizing the open discharge sources for the production of high intensity electron beams with high efficiency. Successful beam generation has been achieved in a variety of operating conditions which include voltages from several hundred to several thousand volts and pulse lengths from tens to hundreds

of nanoseconds with some sources using pulsed power supplies while others operating in self-pulsing mode [12, 19, 20]. In contrast, the source described in this paper operates in a dc steady state quiescent regime. The quiescent regime is suitable for *in situ* study of plasma and surface chemistry [23, 24].

In addition, the scaling of the dc discharge source presented in this paper with $pd \sim 0.3\text{--}1\text{ torr}\cdot\text{cm}$, is similar to the low pd values in the atmospheric pressure microdischarges and hence this source can be used for investigating the use of a steady state plasma source of nonthermal electrons at atmospheric pressure.

The formation of $\sim 100\text{eV}$ electrons and their role in non-local ionization has been studied in short dc discharges since 1980s and continues to be of interest at the present time [5, 25–28]. The short discharges operate without a positive column between two parallel flat electrodes with the distance between the electrodes much smaller than the dimensions of the electrodes. The studies distinguish different groups of electrons including a higher energy group that is produced by secondary electron emission (SEE) from the cathode, and a low energy group produced by the ionization in the negative glow. The ionization is sustained by high energy electrons accelerated in the cathode sheath and arriving to the negative glow region [25, 26]. The plasma-based electron source presented here capitalizes on the non-local character of the EEDF. The non-locality could make it possible to control the electron energy distribution in the regions outside of a millimeter or submillimeter size plasma sources, for example close to the surface of a catalyst used in dry reforming or surface modification. This paper describes the design and characterization of a plasma source of nonthermal electrons. The plasma source has been tested in the pressure range of $2\text{--}10\text{ torr}$ but can be scaled to higher pressures while maintaining a higher ($>10\text{eV}$) energy of the electrons with limited power consumption. Here we report the results for 3 torr operation in gases important for the environmental and biological applications, N_2 , CO_2 , and CO_2/CH_4 mixture.

The outline of this paper is as follows. Section 2, experimental methods describes the design of the plasma source, the set-up, the operating conditions, and the characterization of the source. The results are described in section 3 with a subsection for each, the electrical characteristics of the source, the determination of the electron energies using molecular optical emission spectroscopy (OES), and Langmuir probe results. In section 4, discussion, we estimate the basic plasma parameters of the dc GD plasma source and compare two operations, one with the cylindrical electrode as the anode (CA) and the other with the cylindrical electrode as the cathode (CC) under similar experimental conditions. Finally, we present our conclusions and future plans in section 5.

2. Experimental methods

The breakdown voltage in gasses depends on the product of the discharge pressure, p , and the interelectrode distance, d , or pd . The pd values for the minimum breakdown voltage for CO_2 , N_2 , Ar, and air (gases important for many plasma

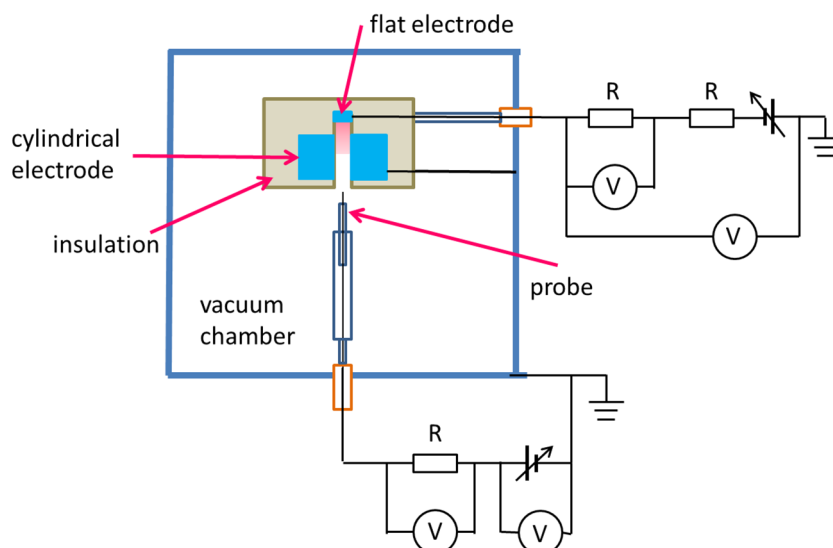


Figure 1. Plasma source design showing the positive high voltage electrode and the grounded cathode. The actual cathode diameter is 1.5 mm. The anode is cylindrical, 1.5 mm in diameter and 3 mm in length. The circuit diagram of the plasma discharge.

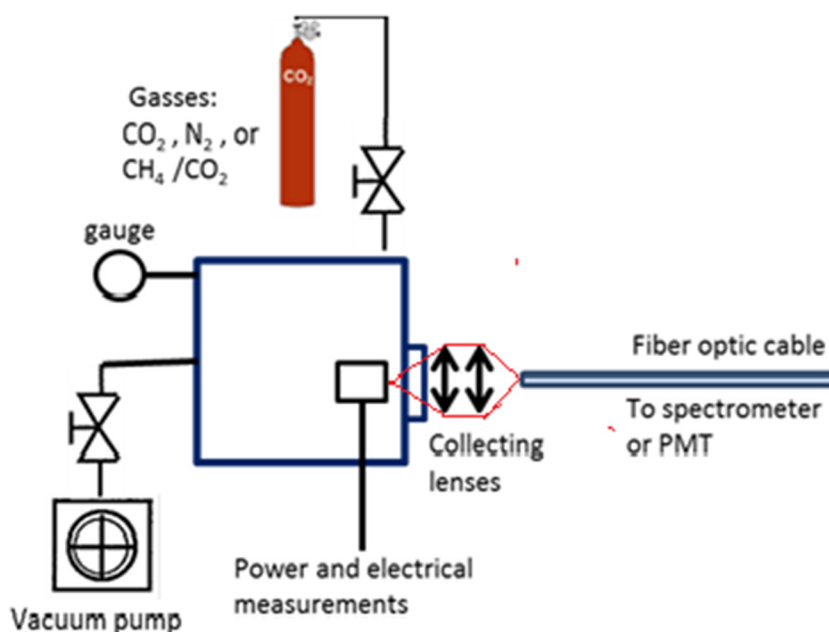


Figure 2. Schematic diagram of the experimental setup.

applications) are in the range of $0.5 \text{ Torr} \cdot \text{cm} < pd < 1 \text{ torr} \cdot \text{cm}$ [10]. The plasma source was designed to operate close to the pd minimum for these gasses. So for a 2–10 torr range, the inter-electrode distance in the device is the 0.1 cm. The plasma source consists of a hollow CA, 1.5 mm inner diameter and 3 mm long, and a flat cathode separated by 1 mm of dielectric material with a 1.5 mm diameter hole (figure 1). The discharge cavity is cylindrical and open to the gas chamber. The pd range is 0.2–1 torr * cm.

The discharge power was supplied by a Bertran 205A-01R high voltage power supply through shunt resistors with a total resistance of $10^5 \text{ k}\Omega$. The current and voltage were measured using a 2 GS s^{-1} Lecroy oscilloscope with a high voltage and a differential voltage probe (figure 1). The plasma source was also operated with the negative voltage applied to the hollow electrode in order to compare the parameters of operation to a more widely used hollow cathode arrangement.

The source was placed in a vacuum chamber, which was evacuated to a pressure of $\sim 10 \text{ mtorr}$ and then filled with a gas of interest maintained at a set pressure in the range of 2–10 torr (figure 2). The pressure was measured by a Baratron gauge. The gasses used in the experiments included CO_2 , N_2 , and 25% CH_4 –75% CO_2 mixture. OES was conducted using an OceanOptics 2000-HR and 4000-UV spectrophotometers. The light collecting optics had a spatial resolution $< 1 \text{ mm}$ and collected light from a region immediately outside of the hollow electrode (figure 2). This is the location of the tip of the Langmuir probe. The stability of the discharge was monitored using a 2 ns rise-time Hamamatsu PMT and an oscilloscope.

OES was used to determine the excitation temperatures of the discharge. The spectra of the discharge in N_2 gas contain rotational-vibrational bands in the UV and visible range corresponding to the electronic transitions of the N_2

neutrals and N_2^+ ions. Specair software package was used to model these bands and determine the rotational, vibrational, and electron excitation temperatures in the discharge [29]. Specair is a collisional radiative model that assumes LTE conditions and a Maxwellian EEDF and includes the transitions relevant to the discharges in air and gasses with the same components such as N_2 or CO_2 . The model generates a spectrum with the chosen transitions and fits the synthetic spectrum to the experimental one by varying the parameters of temperatures and molar concentrations. Due to the computing time, it is not practical to fit all the temperatures at once so the parameters are fitted one at a time, through multiple iterations. Although these assumptions do not hold for plasma that has deviations from Maxwellian EEDF and non-local distribution, the rotational levels are usually in thermal equilibrium with the background gas since the distribution of these levels depends on the collisions with neutrals. The vibrational transitions of the diatomic molecules included in the model are determined by the EEDF of the low energy electrons and are usually also thermalized due to a large collision cross section particularly for N_2 [29].

A Langmuir probe was used to determine the electron energy and plasma density in the region ~ 1.5 mm outside the opening of the hollow electrode (figure 1). The probe was made from a tungsten wire of 0.1 mm in diameter and 2 mm long. The probe was biased relative to the ground using a Kepco BOP power supply. All measurements were taken in a quiescent DC regime. The probe current was determined by measuring the voltage across a 50 k Ω resistor in series with the probe.

3. Results

3.1. Electrical characteristics

The voltage–current (V–I) characteristics were taken for the CA discharge for all three operating gasses in the range of 0.1–10 mA and 200–800 V and for the pressures in the range of 2–10 torr. The current was measured using one of the shunt resistors. The pressure, current, and voltage combination for the operating range was selected for stability of the discharge. The stability of the discharge was verified using a PMT to examine the optical emission from the discharge.

The V–I characteristics shown in figure 3, have a differential resistance of 550–600 k Ω for CO_2 , 450–500 k Ω for N_2 at 3 torr for the CA. The characteristics are similar for the CH_4/CO_2 with the slope of and 500 k Ω under the same conditions (figure 3). The discharge power is in the range of 0.1–0.5 W. In comparison, the differential resistance with reverse polarity, CC arrangement, is 5 k Ω for N_2 and 20 k Ω for CO_2 at 3 torr. At the same pressure, the current range for the CC is up to 10 times greater than the current in the CA configuration and the power supplied is 2–3 times greater for the same driving voltage. For the same pressure and driving voltage, the current density and the voltage between the electrodes are higher in the CA arrangement.

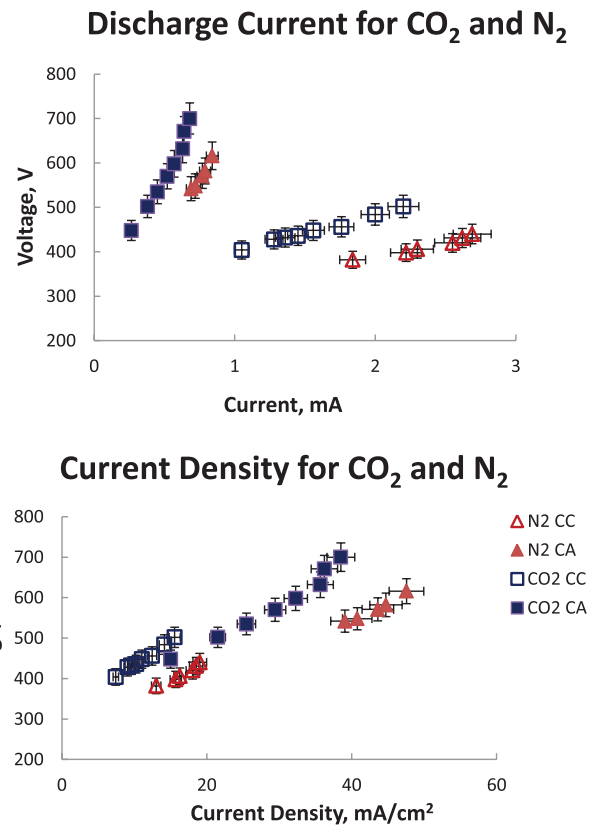


Figure 3. The top graph shows the volt-amp characteristics of the CA and CC arrangements for N_2 and CO_2 working gasses at a pressure of 3 torr. The bottom graph shows the effect of the discharge voltage on the current density for the same conditions.

3.2. Optical emission spectroscopy

OES was conducted in both discharge configurations for CO_2 , N_2 , and CH_4/CO_2 mixture. The spectra are shown here for the 3 torr operating pressure (figure 4). OES was conducted using a lens with a 1 mm length focal plane, focused about 1 mm outside of the cathode or the anode opening. The bands corresponding to the transition from $N_2(C^3\Pi_u)$ to $N_2(B^3\Pi_g)$ state, the so-called, second positive system are well represented in the spectra of both configurations with strong band heads at 337.1 nm, 357.7 nm, 380.5 nm, etc (figure 4). The bands corresponding to the N_2^+ ion first negative system ($B^2\Sigma_u^+$ to $X^2\Sigma_g^+$) are also visible with strong peaks at 391.4 nm, 427.8 nm, for example. The spectra show clear differences in the intensity of the N_2^+ ion emission bands relative to the intensity of the bands of the N_2 neutral molecule:

$$\text{For HC : } \frac{I_{391\text{nm}}}{I_{380\text{nm}}} = 1.3, \text{ while for CA, } \frac{I_{391\text{nm}}}{I_{380\text{nm}}} = 4. \quad (1)$$

Similar intensity ratios were observed in the spectra with CO_2 as the operating gas with N_2 as an impurity. The discharges in CO_2 and CH_4/CO_2 mixture in addition to the molecular bands (ex, CO Angstrom bands) have atomic lines such as the 777 nm line characteristic for the atomic Oxygen, and the 656 nm H_{α} , Balmer series line. The spectra indicate a higher degree of dissociation of the operating gas in the CA

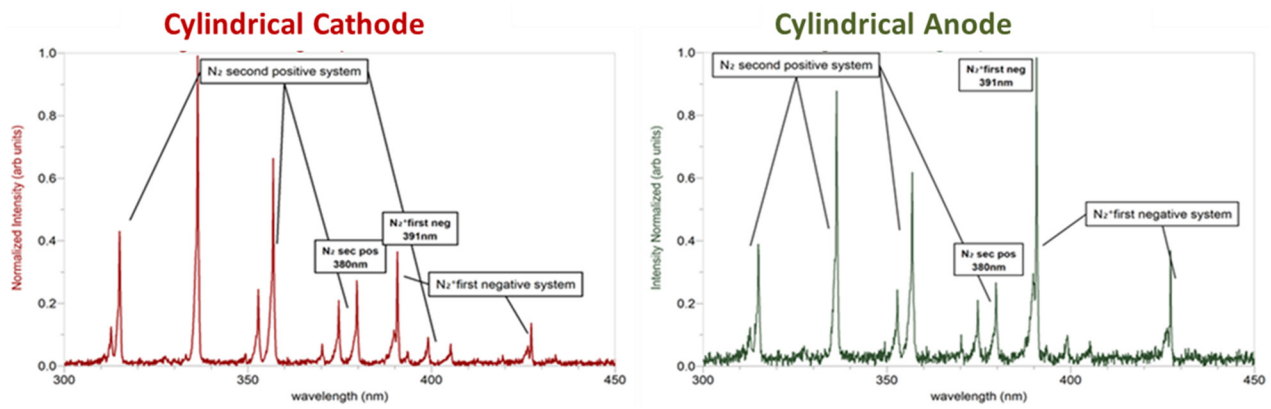


Figure 4. The OES show strong changes in the intensity of the N_2 ion emission bands relative to the intensity of the bands of the N_2 neutral molecule.

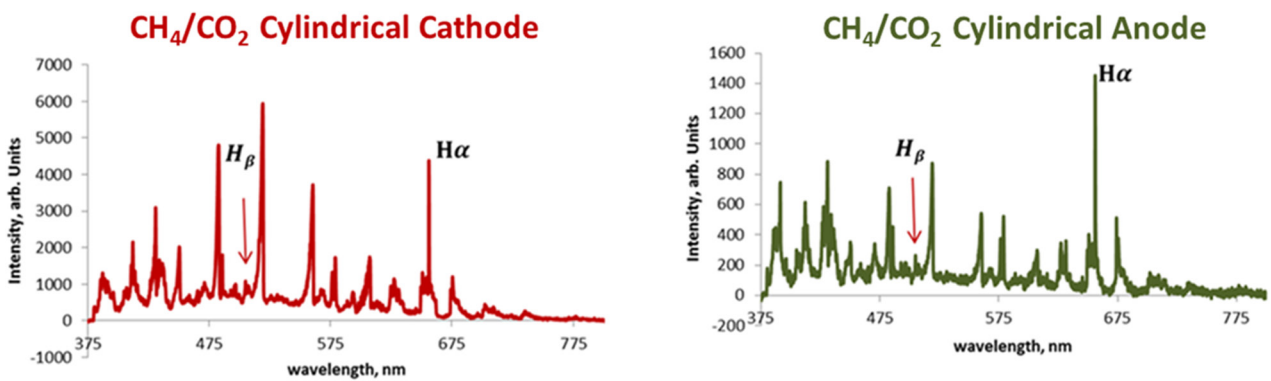


Figure 5. OES spectra for CH_4/CO_2 operation in CC configuration (left) and CA configuration (right). The spectra show a much higher degree of decomposition of methane in the CA arrangement than HC as evident from the dramatic increase in the H_α emission. The H_β emission is difficult to isolate but it also shows a relative increase in intensity.

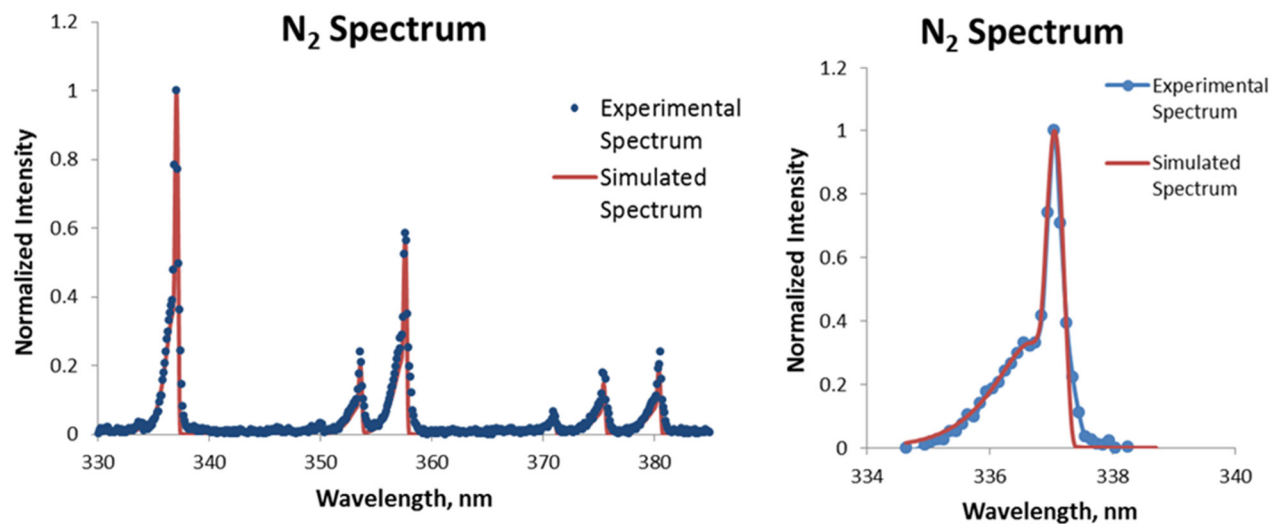


Figure 6. SpecAir fit to N_2 vibrational band spectrum of the second negative system (left) and the unresolved 337 nm band of this system.

configuration as seen by a higher proportion of the emission due to the atomic fragments, such as H and O, than in the CC arrangement (figure 5).

Specair spectrum fitting software was used to determine the rotational and the vibrational excitation temperatures of N_2 discharge. Two N_2 unresolved vibrational/rotational bands, 337.1 nm and 357.7 nm, were isolated and used in separate trials

to determine the rotational excitation temperature (figure 6). The rotational excitation temperature for the voltage/current conditions shown in figure 3, increased from 440 ± 10 K to 500 ± 10 K with increasing voltage for the CA. The CC configuration had a higher rotational excitation temperature which varied from 480 ± 10 K to 530 ± 10 K with increasing discharge current. The vibrational excitation temperatures were determined

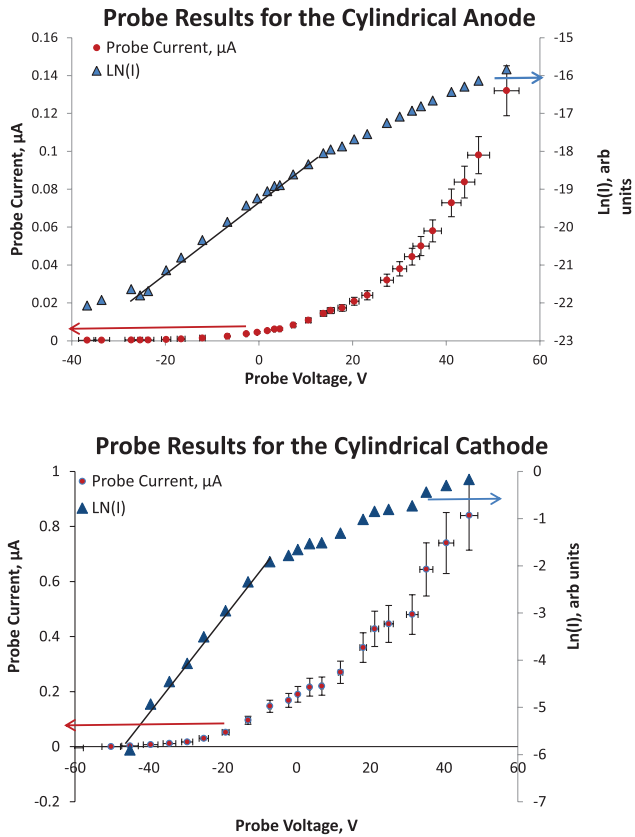


Figure 7. Langmuir probe measurements for the CA and CC arrangements. The straight line segments on the logarithmic plots indicate the regions of the I–V characteristic used to determine the electron temperature, 12–15 eV for the CA and 9–10 eV for the CC.

by fitting a spectrum containing several N₂ vibrational bands from the second positive system. The Specair fitting results gave higher vibrational temperatures for the CA configuration, for example, 4500 K for the CA and 3700 K for the HC configuration (figure 6). The determination of the electron temperature, T_e, would require a model that can take into account the non-equilibrium conditions with low and high energy electrons present in the plasma. Specair is not intended for such applications.

3.3. Langmuir probe results

The Langmuir probe was positioned as shown in figure 1 for both CA and CC arrangements, effectively within the plasma plume for the CC arrangement. In case of the CA the discharge was confined to a region close to the flat negative electrode which is about 4–6 mm from the probe for the same location of the probe. Sample probe I–V characteristics for the CA and the CC electrode arrangements are shown in figure 7. If the electron distribution is Maxwellian, the semi-log plot of the probe current versus voltage exhibits a linear segment and the electron portion of the current is given by [26]:

$$I_e = I_{es} \exp \left[\frac{V - V_p}{T_e} \right]. \quad (2)$$

Where V is the probe voltage relative to ground, V_p is plasma potential, T_e is the electron temperature in eV and I_{es} is the electron saturation current, [24],

$$I_{es} \approx en_e A_p \sqrt{\frac{e T_e}{m_e}}.$$

The electron temperature can be determined from the slope of the semi-log plot (figure 7). The somewhat collisional nature of the plasma outside of the source in the pressure range of 2–10 torr complicates the analysis of the probe characteristics, but the straight portion of the log I versus V plot remains useable for the determination of the T_e as long as the density remains relatively low and the plasma is far from LTE [30, 31]. Applying this method to the probe characteristic in our experiment results in values of T_e > 10 eV. The values obtained from the slope are in the range of 12–15 eV and for the CA arrangement and 9–10 eV for the CC arrangement. The probe characteristics do not saturate and the ion saturation current is below the reliable detection level of the micro-voltmeter used to measure the current from the probe (figure 1). Given the approximate probe current in the range of 0.1–0.8 μA, an order of magnitude estimate of the plasma density in the area of the probe for T_e ~ 10 eV gives n_e ~ 10⁷–10⁸ cm⁻³.

4. Discussion

The plasma source was operated in two geometric configurations, one with a CA and the other in reverse polarity, with the cylindrical electrode serving as the cathode. Both arrangements operate as GDs in the abnormal regime that is with a positive slope V–I curve (figure 3) which is a stable quiescent glow regime. The current density dependence on voltage is also typical for a GD. Although the focus is on the conditions outside of the plasma source and OES and probe measurements tested that region, some discussion of the properties inside the plasma source is necessary (figure 1).

4.1. Inside a plasma source

Unlike the Grimm discharges, the current in the CA arrangement is limited to a few milliamps. For N₂ as the plasma gas, the discharge voltage increases from 400 V to 800 V as the discharge current increases from about 0.5 mA to 0.7 mA for the CA configuration while for the CC case, the voltage increases by about 10 V when the current increases from 1 mA to 3 mA. The highest operating power was about two times higher for the CC than the CA arrangement and hence the CC discharge was brighter, had higher gas temperature and produced a bright plume outside of the CC. These parameters are closer to the dc GD in N₂ that has been studied mostly in a parallel-plate geometry, and typically has the plasma density of about 10⁹–10¹⁰ cm⁻³ and a temperature under or around 1 eV [1]. Since the small size of our plasma source makes the investigation of the properties inside the discharge difficult, we will assume that the typical values apply to our discharge and make some simple estimates to gain some insight into the nature of this plasma source.

As shown in figure 3, the current density was higher in the CA arrangement than in the CC arrangement due to a smaller area of the cathode. The flat electrode area was 0.018 cm²

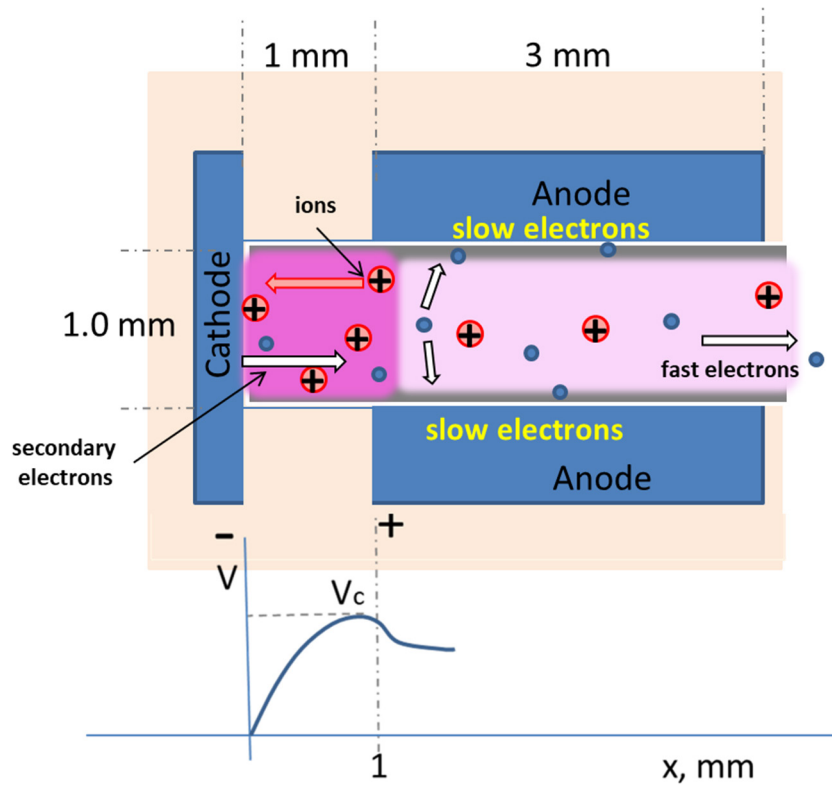


Figure 8. A diagram of some of the discharge processes inside the plasma source.

and the cylindrical electrode area was 0.14 cm^2 . For the same applied voltage of 600 V to 800 V, the current density to the cathode, j_c , varied from 13 mA cm^{-2} to 19 mA cm^{-2} for the CC arrangement and from 37 mA cm^{-2} to 47 mA cm^{-2} in the CA arrangement. In CA, the increase in current density was achieved with a much higher increase in the potential difference between the electrodes. In a cold-cathode GD the cathode current is generated by the flow of ions to the cathode and secondary electrons produced by the ion bombardment of the cathode (so-called ion-induced SEE) [1]:

$$j_c = en_i v_{id} (1 + \gamma_e).$$

Where j_c is the current density at the cathode, e is the electron charge, n_i is the ion density, v_{id} is ion drift velocity and γ_e is the SEE yield from the cathode material for the gas ions. Since the ion density and drift speed depend on the cathode sheath potential, V_c and the length of the cathode sheath, d_c , for a given ion mobility, and coefficient of SEE, γ_e , the current density depends on both, V_c and d_c .

In a normal GD the cathode region adjusts to the pd_{\min} for the given gas, but in an abnormal glow, the voltage drop in the cathode sheath can take a large portion of the applied voltage and the cathode length can increase. The normal cathode voltage drop for a GD in N_2 is $V_n \sim 200 \text{ V}$ [1]. For a simplified assumption of a uniform charge density in the sheath, the sheath length can be estimated as $d_c = \lambda_D \sqrt{\frac{2V_c}{T_e}}$ giving a cathode sheath thickness at least several times and up to an order of magnitude longer than the Debye length.

For the typical parameters of a GD in a nitrogen gas, (10^9 – 10^{10} cm^{-3} and $\sim 1 \text{ eV}$) the Debye length is of the order of 0.1 mm, hence the sheath length is close to 1 mm, which is the distance between the electrodes (see figures 1 and 8). The cathode pd_{\min} for N_2 and Ni cathode was not available, but the SEE coefficients for Ni and Fe are close, and pd_{\min} for Fe cathode and N_2 gas is $0.42 \text{ torr} \cdot \text{cm}$ confirming our estimates of $pd_c \approx 0.3 \text{ torr} \cdot \text{cm}$.

These estimates mean that the discharge in our plasma source operates without a positive column and may be an obstructed discharge. In an obstructed discharge, $pd_c < pd_{\min}$, the distance between the electrodes too small for normal multiplication, and an increase in voltage between the electrodes is needed to maintain the GD. The voltage of the cathode sheath varies as a square root of the current density, hence

$$\frac{V_c}{V_n} = \sqrt{\frac{j_c}{j_n}}$$

where j_n is the normal current density for the given gas and cathode material. For N_2 with either Ni or Fe cathode, $\frac{j_n}{p^2} = 0.4 \text{ mA cm}^{-2} \text{ torr}^2$ [1], giving a normal current density of $j_n = 3.6 \text{ mA cm}^{-2}$. For our measured current densities, this gives an estimated cathode voltage in the range of ~ 400 – 500 V for the CC case and 600 V – 700 V for the CA arrangement, and an estimated reduced field, E/p in the range of $\text{kV cm}^{-1} \cdot \text{torr}$. Electric fields of this magnitude can be expected to produce high energy electrons. The collisional nature of this discharge and the high collision cross sections for N_2 vibrational

transitions are going to thermalize a low energy component of the electron population leaving one or more groups of non-equilibrium and non-local high energy electrons [32–37].

It is typical for short discharges that most of the discharge voltage falls in the cathode sheath [25, 26], therefore the higher discharge voltage in the CA arrangement would produce higher energy electrons. The SEE electrons from the cathode accelerate in the cathode sheath towards the negative glow region gaining the energy equal to the sheath voltage eV_c , where e is the electron charge. In the negative glow region these energetic electrons become the main sources of ionization of the neutrals. Hence, several electron energy groups exist in the discharge, the fast electrons accelerated through the cathode sheath, the medium energy group that consists mostly of the slowed fast electrons, and the low energy electrons produced by the ionizations in the negative glow. The low energy electrons form the largest group, determine the overall plasma density and temperature between the electrodes, but may become trapped in the negative glow due to field reversal [25, 26, 43].

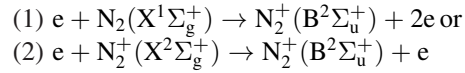
In addition to the electron acceleration in the cathode sheath, the anode sheath may have an accelerating or a retarding effect on the electrons. Accelerating anode potential has been found responsible for the production of electrons with energies of the order of the ionization potential of the plasma gas, 15.6 eV for N_2 . Experimentally and theoretically, it has been shown in many investigations [1, 7, 38–40] that GDs tend to have various groups of electrons, cooler thermalized electrons of a few eV or below, a group of higher energy ionizing electrons, and high energy beam electrons. It is the presence of the higher energy non-local electrons that makes it possible to use this plasma source as an electron source. The main problem becomes extracting these electrons from the source. A simple way of allowing electrons to escape is making a hole in the electrode. In case of the CA it is the anode that has a hole, and in the opposite polarity, the cathode.

4.2. Outside the plasma source

Now we focus on the region outside of the anode opening or in reverse polarity, the cathode opening. Visually, the CA arrangement had a lower overall emission intensity than the CC arrangement and a barely visible plume. Emissions from both discharge arrangements were investigated using OES and a Langmuir probe. The measurements provide some evidence that CA arrangement is a source of higher energy electrons than the CC arrangement although plasma density appears to be higher in the plume of the CC source.

The analysis of N_2 vibrational spectra showed higher vibrational excitation temperature, $T_{vib} \approx 0.4$ eV, for the CA discharge than CC, where $T_{vib} \approx 0.3$ eV. Although SpecAir spectrum simulation program assumes LTE, it gives good results for the vibrational and rotational transitions because the vibrational and rotational transitions usually are in LTE. The higher rotational temperature in the CC discharge indicates more intense gas heating in this configuration. The spectra for nitrogen in CA configuration show a relatively

higher intensity of N_2^+ first negative system than in CC. The increased emission intensity of N_2^+ ion requires ionization of the N_2 molecule (ionization energy of 15.6 eV) and the production of the ion excited state, for example through direct ionization of N_2 into an excited state or through the excitation of a nitrogen ion from its ground state:



The threshold electron energy for the direct ionization and excitation of nitrogen from the ground state $N_2(X^1\Sigma_g^+)$ is 18 eV (reaction 1 above) [41]. The second reaction requires electron energies in the single eV but it also requires electron-ion collisions that become significant only at high degree of ionization. Therefore, the first channel (1) is favored when there is a greater population of high-energy electrons and channel (2) is favored at high plasma densities. Since the densities in GD are relatively low, a relatively high N_2^+ emission intensity indicates higher electron energy in the CA configuration [32–34]. The OES of the other gasses corroborates this conclusion. The spectra of the discharge in CO_2 and CH_4/CO_2 mixture show a higher intensity of the O and H atomic lines. This requires a higher degree of decomposition of the molecular gasses. CO_2 decomposition requires electrons with energies >10 eV and reduced electric fields of the order of $60 \text{ V cm}^{-1} \cdot \text{torr}^{-1}$ [34]. Although it is difficult to eliminate all the light from the inside of the source the OES results indicate the presence of >10 eV electrons in the region outside of the discharge. These results were corroborated by Langmuir probe measurements with the probe positioned at the same location, ~ 2 mm outside of the discharge.

At this location, the probe is clearly immersed in the plume from the CC discharge. It is more difficult to establish if the same is true for the CA because of the low emission intensity. The analysis of the first exponential increase in the Langmuir probe current shows the presence of nonthermal medium-energy electrons in both CA (12–15 eV) and CC (9–10 eV) discharge with higher electron energies in the CA discharge. The Langmuir probe measurements for this discharge are challenged by the small size of the device, the collisional nature of the discharge, and the presence of electrons of various energies including non-thermalized beam electrons, and low plasma density. The first exponential increase in the probe current in this collisional environment corresponds to the probe collecting the high energy electrons. The interpretation of this section still holds even though it cannot be interpreted as the temperature of the plasma electrons in the discharge. The Langmuir probe results indicate the presence of nonthermal electrons in the region ~ 5 mm from the cathode for the HA arrangement and indicate the nonthermal energy component of the plasma generated at the location of the probe.

Although the results from the OES and Langmuir probe measurements support the presence of nonthermal electrons outside of the discharge, with higher energy electrons produced in the CA discharge, the results require additional measurements using energy analyzer to determine the energy spectrum of the electrons produced by the plasma.

Table 1. Some parameters for the plasma source. The estimates are for the operating pressure of 3 torr with the ranges given for 2–10 torr.

	Conductivity, $10^{-5}\Omega^{-1}\text{cm}^{-1}$	Electron density, 10^{10}cm^{-3}	Reduced electric field, $\text{V cm}^{-1} \cdot \text{torr}^{-1}$	Debye length, $\lambda_D \mu\text{m}$
CA	1	1	10^3	$10^1\text{--}10^2$
CC	10	10		

Table 2. Characteristic distances in N_2 at 3 torr.

Electron energy	Mean free path, electron-neutral collisions, λ , mm	Energy relaxation through elastic collisions, λ_{el} , mm	Energy relaxation distance through inelastic collisions, λ^* , mm
1–3 eV	10^{-2}	1	10^{-1}
15 eV	10^{-1}	10	1

4.3. Plasma source of electrons

Can we expect beam electrons in the 2–10 torr pressure range of our experiments? What is the interplay between plasma parameters and the size of the plasma source? The presence of beam electrons is important for targeted applications for both gas and surface chemistry. In the CA arrangement the discharge is confined to the region close to the flat electrode (figure 1) so would it be possible to extract the high energy electrons to the regions where these electrons could do useful work? Is it possible to use the non-local effects for creating radicals and sustaining plasma chemical reactions in a region outside of the immediate discharge region?

Estimations of the sheath size and energy relaxation distance are shown in tables 1 and 2 together with the estimations discussed above. The energy relaxation distances [35] are comparable or greater than the size of the discharge. Therefore, non-equilibrium conditions should be expected as supported by the OES data. In addition, if high energy electrons are present, these electrons may not thermalize within the confines of the discharge. The non-equilibrium and non-local conditions have been investigated in many studies of GD for a variety of pressures and other discharge conditions [30, 34–37]. Non-thermal electrons may be used outside of the discharge (provided a suitable extraction scheme) for modifying surfaces or for specific ‘resonant’ reactions.

The CA arrangement has a voltage difference up to 700–800 V for an inter-electrode distance of 1 mm, resulting in high electric fields and a production of energetic electrons as discussed above, including electrons with energies $> 10\text{eV}$ in the range of the first electron excitation of N_2 . In N_2 gas, the total collision cross section peaks at about, $\sigma \approx 30 \times 10^{-16}\text{cm}^2$ [39] for electrons in the 1–3 eV energy range due to the electron impact excitation of the molecular vibrational states, but drops considerably for electrons $> 10\text{eV}$. The corresponding mean free path for electrons in the 1–3 eV range is $\lambda \approx 0.03\text{mm}$ and $\lambda \approx 0.1\text{mm}$ for the 15 eV electrons. Since these distances are shorter than the inter-electrode distance, plasma in the source is collisional in nature, but does not ensure thermalization of all electron populations. Elastic energy relaxation distances are longer than the mean free path by a factor of $\sim \sqrt{\frac{2m}{M}} \approx 125$, where m is the mass of an electron and M is the mass of a nitrogen

molecule, giving distances of $\sim 4\text{mm}$ and 12mm for the lower and higher electron energies, respectively. The inelastic energy relaxation length $\lambda^* \approx \lambda \sqrt{\frac{\nu}{\nu^*}}$, where ν and ν^* are elastic and inelastic collision frequencies [26] which gives $\lambda^* \approx 3\lambda$, for the 1–3 eV electrons and $\lambda^* \approx 10\lambda$, using the values for collision cross sections in [42]. The 1–3 eV electrons can be thermalized within the source, with $\lambda^* \approx 0.1\text{mm}$ as expected for molecular gases. On the other hand, the inelastic energy relaxation length is $\sim 1\text{mm}$ for the 15 eV electrons, which is of the same order as the size of the source. According to [43] one can expect that $\lambda^* \approx 100\lambda$ for $pd < 10\text{ torr} \cdot \text{cm}$, and in the experiments described here this holds in all conditions, and at 3 torr, $pd = 0.3\text{ torr} \cdot \text{cm}$. The energy relaxation distances for the elastic and the inelastic electron-neutral collisions are shown in table 2. The estimated distance for 15 eV is comparable with the axial size of the discharge therefore, it is reasonable to expect electrons with energies $\sim 15\text{eV}$ to be present in a region greater than the size of the source provided these electrons are not collected by the anode. The differential cross section for electron-neutral collisions is more isotropic for the lower energy electrons, $< 5\text{eV}$, than for the higher energy electrons. The differential cross sections for the elastic and inelastic collisions of electrons with neutrals decrease rapidly for higher angles for electrons with the energy in 10–100 eV and higher [27, 28]. As a result, the higher energy electrons are scattered forward, i.e. preferentially along the direction of the accelerating electric field [5, 25–28]. This scattering anisotropy makes it possible for the higher energy electrons to pass through the anode opening while the lower energy electrons are either trapped in the negative glow or scattered by collisions and collected by the anode. Therefore, it is reasonable to expect higher energy electrons outside of the opening of the plasma source, while lower energy electrons are conducting the current to the anode. Since the measured energy of the fast electrons is above the excitation levels of the gas molecules, collisions outside of the source may lead to further thermalization of these electrons, so the measured electron energy is expected to decrease with the distance from the source. These electron kinetics processes require modeling which will be addressed in future studies.

There is no gas flow in our system and the plasma exits the CC discharge due to a higher gas temperature and due to the negative potential of the cathode with respect to the

surrounding chamber. In case of the CA, a negative anode voltage is much lower, of the order of 1 eV, the temperature of the low energy electrons for the low current GD situation such as ours and does not [1, 25, 44], and a plume is not observed. As stated above, the Langmuir probe results and OES indicate that electron energy is lower and plasma density and gas temperature are higher outside of the CC source than the CA source. In case of the CA source, the opening is in the anode, hence allowing the electrons approaching the anode to escape (figure 8). During the passage through the cylindrical opening in the anode, the lower energy electrons sink into the anode, while the higher energy, or possibly, beam electrons escape through the opening. The anode opening serves as an energy filter for the exiting electrons. The CA configuration and its possibilities for the control of the energies of the exiting electrons warrant additional investigations to (1) establish how the anode geometry affects the energy of the electrons, and (2) to analyze the energy distribution of these electrons.

The non-local characteristics of the plasma source described here are the consequence of the pd scaling of this device. If the pd is increased, the relaxation lengths would become smaller than the inter-electrode distance, the discharge would become more collisional and tend to local equilibrium. At an increased distance, the discharge will acquire a positive column where the ionization balance depends on the local reduced electric field, E/p , and the beam components of the EED would not be able to reach the outside of the source. At lower pressure, it would not be possible to maintain a cold cathode discharge without increasing the area of the cathode. Maintaining the same pd, it is possible to scale the device to higher pressures by reducing the size of the device, but the operation at the microscale requires more detailed studies including modeling.

A plasma source of electrons with energies in a 10–20 eV range is important for precision control of gas phase chemistry, such as for example, CO₂ decomposition or methane reforming, and for plasma surface modification [44–46]. Previous works had focused on maximizing the power of the electron or ion beams and not on targeting specific bond energies [47–49]. The device proposed here could be used to increase control over plasma treatment.

5. Conclusions

We have developed a plasma source of nonthermal electrons based on a non-local, non-equilibrium GD, a GD that can be used as a source of nonthermal electrons and opens possibilities for control or selection of the energy of the electrons that exit the source. Operating in a dc quiescent regime, the source is suitable for *in situ* studies of targeted gas and surface chemistry. The non-equilibrium and non-local nature of the GD leads to the existence of high energy electrons. The electrons are produced by ion SEE and accelerated in the cathode potential. The geometry of the source eliminates the thermalized positive column and allows the high energy and possibly beam electrons to escape the discharge cavity. The cylindrically shaped anode allows the high energy electrons to

escape while absorbing the lower energy electrons as shown in figure 8. Hence, the anode opening serves as an energy filter for the exiting electrons. This suggests a possibility of controlling the energy of the exiting electrons by varying the geometry of the anode.

Our estimates confirm the non-locality and confined nature of the discharge and our experiments confirm the presence of high energy electrons, 12–15 eV outside of the opening of the CA.

Additional studies are needed to further characterize the emitted electrons and to establish control of their properties possibly using the discharge geometry. The control of the energy is particularly important for chemical processes such as the examples given here of the decomposition of carbon dioxide and methane reforming. Future studies will also focus scaling of this plasma source of high energy electrons based on a non-equilibrium GD, for operation at higher pressures.

Acknowledgments

The authors thank Alex Merzhevsky and Kevin Pardinias for their assistance with experiments, Bruce Koel for motivating these efforts with application to plasma surface chemistry, and Mikhail Shneider and Dima Levko for fruitful discussions of our results. We are grateful to Igor Kaganovich, Vladimir Demidov, Sergey Macheret, Alexander Mustafaev, and Irina Schweigert for bringing to our attention the non-equilibrium microplasmas and open discharges.

This work was supported by US DOE U.S. Department of Energy, Office of Science, Fusion Energy Sciences, Contract No. DE-AC02-09CH11466 and AFOSR.

ORCID iDs

S Gershman  <https://orcid.org/0000-0002-8409-4029>

Y Raitses  <https://orcid.org/0000-0002-9382-9963>

References

- [1] Raizer Y 1997 *Gas Discharge Physics* (New York: Springer)
- [2] Phelps A 1999 *Plasma Sources Sci. Technol.* **8** R21–44
- [3] Bogaerts A 1999 *J. Anal. At. Spectrom.* **14** 1375–84
- [4] Kudryavtsev A *et al* 2012 *Tech. Phys.* **57** 1188–91
- [5] Carlsson J *et al* 2016 *Plasma Sources Sci. Technol.* **26** 014003
- [6] Schoenbach K and Becker K 2016 *Eur. Phys. J. D* **70** 29
- [7] Adams S F *et al* 2016 *Phys. Plasmas* **23** 24501
- [8] Smy P R 1976 *Adv. Phys.* **25** 517–53
- [9] Burdovitsin V and Oks E 2008 *Laser Part. Beams* **26** 619–35
- [10] Benilov M S 2000 *J. Phys. D: Appl. Phys.* **33** 1683–96
- [11] Lock E H *et al* 2010 *Langmuir* **26** 8857–68
- [12] Bobrov V A *et al* 2013 *Tech. Phys.* **58** 1205–10
- [13] Lisovskiy V, Artushenko K and Yegorenkov V 2017 *Phys. Plasmas* **24** 053501
- [14] Bogdanov E *et al* 2010 *Phys. Plasmas* **17** 103502
- [15] Barnat E, Laity G and Baalrud S 2014 *Phys. Plasmas* **21** 103512
- [16] Bogaerts A and Gijbels R 1998 *Spectrochim. Acta B* **53** 437–62

- [17] Bogaerts A *et al* 2004 *Spectrochim. Acta B* **59** 449–60
- [18] Gamez G *et al* 2004 *Spectrochim. Acta B* **59** 435–47
- [19] Bokhan A P and Bokhan P A 2001 *Tech. Phys. Lett.* **27** 220–2
- [20] Bokhan A P, Bokhan P A and Zakrevsky D É 2005 *Appl. Phys. Lett.* **86** 151503
- [21] Bokhan A P, Bokhan P A and Zakrevsky D É 2006 *Plasma Phys. Rep.* **32** 549–62
- [22] Belskaya E V, Bokhan P A and Zakrevsky D É 2008 *Appl. Phys. Lett.* **93** 091503
- [23] Gershman S, Raitses Y, Paradinas K and Koel B 2016 Reactive microplasma discharge for *in situ* study of surface modification *69th Gaseous Electronics Conf. (Bochum, Germany, October 2016)*
- [24] Raitses Y and Gershman S 2017 Generation of energetic electrons in a plasma source at fore-vacuum pressures *APS 70th Annual Gaseous Electronics Conf. (Pittsburgh PA, October 2017)* p 6210
- [25] Tsendin L D 1995 *Plasma Sources Sci. Technol.* **4** 200
- [26] Kolobov V I and Tsendin L D 2008 *Tech. Phys.* **53** 1029–40
- [27] Linert I and Zubek M 2009 *J. Phys. B: At. Mol. Opt. Phys.* **42** 085203
- [28] Gao J, Madison D H and Peacher J L 2005 *Phys. Rev. A* **72** 020701
- [29] Laux C O 2008 2008 Optical diagnostics and collisional-radiative models *VKI Course on Hypersonic Entry and Cruise Vehicles (Stanford University, 30 June–3 July 2008)*
- [30] Swift J D and Schwar M J R 1969 *Electrical Probes for Plasma Diagnostics* (London: Iliffe Books)
- [31] Godyak V and Demidov V 2011 *J. Phys. D: Appl. Phys.* **44** 233001
- [32] Isola L, Gomez B and Guerra V 2010 *J. Phys. D: Appl. Phys.* **43** 015202
- [33] Qayyum A, Zeb S and Ali S 2005 *Plasma Chem. Plasma Process.* **25** 551
- [34] Dalvie M, Hamaguchi S and Farouki R 1992 *Phys. Rev.* **46** 2
- [35] Demidov V *et al* 2016 *Phys. Plasmas* **23** 103508
- [36] Petrov G and Winkler R 1998 *Plasma Chem. Plasma Process.* **18** 1
- [37] Spasojevic D *et al* 2012 *Plasma Sources Sci. Technol.* **21** 025006
- [38] Lucas J 2001 *High Voltage Engineering* (Sri Lanka: University of Moratuwa)
- [39] Gleizer J *et al* 2005 *J. Phys. D: Appl. Phys.* **38** 276–86
- [40] Dorf L, Raitses Y and Fisch N 2005 *J. Appl. Phys.* **97** 103309
- [41] Sanderson R 1976 *Chemical Bonds and Bond Energy* 2nd edn (New York: Academic)
- [42] Itikawa Y 2005 *J. Phys. Chem. Data* **35** 31–53
- [43] Demidov V I 2005 *Phys. Rev. Lett.* **95** 215002
- [44] Smirnov B M 2015 *Theory of Gas Discharge Plasma* (Berlin: Springer)
- [45] Locht R and Davister M 1995 *Int. J. Mass Spectrom. Ion Process.* **144** 105–29
- [46] Castell R *et al* 2004 *Braz. J. Phys.* **34** 4B
- [47] Srivastava M and Kobayashi A 2010 *Trans. JWRI* **39** 11–25
- [48] Masayuki F *et al* 2000 *Vacuum* **59** 358–72
- [49] Hassan A *et al* 2007 *Rev. Sci. Instrum.* **78** 123301